A New Expandable Detector Applied to Digital Topography and TM Image Data in Support of Petroleum Exploration*

Richard L. Thiessen, Khalid Soofi, and Hans Sheline

Abstract

Washington State University (WSU) is developing a series of analysis packages that detect faults and fractures in a variety of digital databases. Our automated lineament analysis program, NODES, uses a unique counting circle approach to find linear structures. The circle's diameter can range from 3 to 91 pixels. Each pair of symmetrically opposite points within the circle is tested against its center to find anomalous points. This detector can find light or dark lineaments, image gradients, gradient breaks, and topographic ridges, valleys, slopes, and slope breaks.

Here we present results of using NODES in a southeastern New Mexico test area. The area is characterized by a set of northwest lineaments parallel to broad valleys that were not delineated by a 15-pixel valley detector, but were by a 41-pixel one. Darker lineaments and gradients, 31 pixels across, were found on TM band 7 data as were topographic slopes and subsurface gradients. A field check of one showed it to be a contact, possibly a fault. A regional low, found with the 91-pixel valley detector, is an area of evaporite dissolution, controlled by the edge of the Capitan reef. In the region to the north the overlying lithologic layers drape across the reef and expand into this dissolution zone, causing the valley lineaments.

Introduction

Faculty and students at Washington State University (WSU), in conjunction with staff from the Pacific Northwest Laboratory, are developing a series of comprehensive, computer automated fracture analysis packages. Our Geologic Spatial Analysis (GSA) programs automatically detect evidence for geologic faults and fractures in a variety of digital databases, including topography, remotely sensed images, depths to subsurface interfaces, earthquake foci, and geophysical data bases. The methods examine the alignment of data in three

dimensions, yielding the location and orientation (strike and dip) of any possible geologic structures. One of these programs, NODES, automatically defines lineaments on topographic, image, geophysical, and subsurface databases. Conoco, as part of their support of advanced methodologies, provided extensive databases to be analyzed with the system. A study area in the southeast corner of New Mexico was selected, as shown in Figure 1. Two adjacent Landsat Thematic Mapper (TM) images had previously been acquired. Well developed northwest-oriented lineaments which correspond to valleys had been noticed on one of the TM images. Digital elevation models at 1:24,000 scale were purchased from the U.S. Geological Survey (USGS). Because the study area is within the Delaware Basin, extensive well control exists, and a number of plots of depths to subsurface interfaces were available. Studied stratigraphic intervals include the top of undifferentiated Silurian-Devonian, Morrowan, Wolfcamp, Yates, Capitan, Castile, Salado, Rustler, top of undifferentiated Redbeds, Post-Mesozoic erosional unconformity, bedrock highs, groundwater table, Tertiary mafic dikes, Tertiary basins, faults mapped at the surface, and topographic scarps.

Project Area

The Hobbs project area (Figure 1) is the New Mexico portion of the Hobbs 1:250,000-scale topographic (USGS, 1973) and geologic (Barnes, 1976) map sheets. It extends from 104° W longitude to the Texas-New Mexico border, and from a latitude of 32° N to 33° N. The selected study area, designated the Querecho Plains (QP) area (Figure 1), includes the series of well developed northwest-oriented lineament valleys. The northwest corner of QP is at 103° 53' 50" W and 32° 51' 12" N latitude. The bounds in UTM (Universal Transverse Mercator) zone 13 are 603,180 to 647,070 m E and 3,579,330 to 3,635,400 m N. QP has a topographic elevation range of 182 m. The Grama Ridge (GR) detailed study area (Figure 1) was defined in order to be able to analyze full resolution color plots of the results using a standard page sized color printer. The UTM limits of Grama Ridge (GR) are 631,380 to 640,380

Richard L. Thiessen, Geology Department, Washington State University, Pullman, WA 99164-2812.
Khalid Soofi, Remote Sensing Laboratory, 2402 RDW, Conoco, Inc., Ponca City, OK 74603.
Hans Sheline, Exploration Division Office, Conoco Midland, 10 Desta Drive West, Midland, TX 79705. Present address, P.O. Box 2222, Dubai United Ariab Emerites, Arabian Gulf.
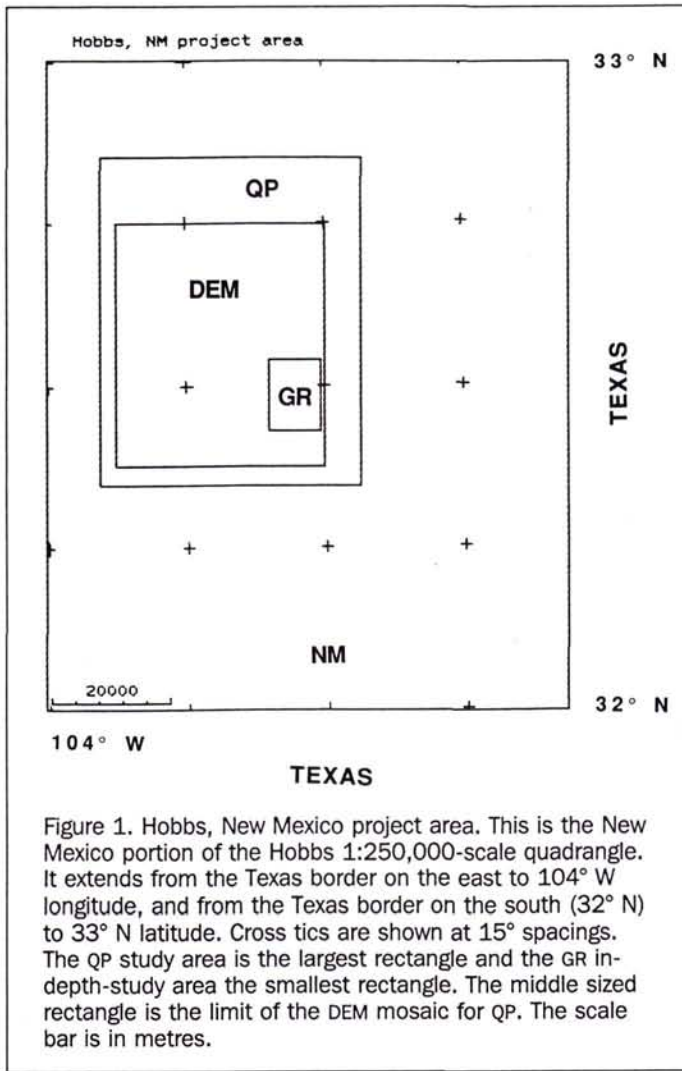

Figure 1. Hobbs, New Mexico project area. This is the New Mexico portion of the Hobbs 1:250,000-scale quadrangle. It extends from the Texas border on the east to 104° W longitude, and from the Texas border on the south (32° N) to 33° N latitude. Cross tics are shown at 15° spacings. The QP study area is the largest rectangle and the GR in-depth-study area the smallest rectangle. The middle sized rectangle is the limit of the DEM mosaic for QP. The scale bar is in metres.

m E and 3,588,930 to 3,600,930 m N. **GR** exhibits 84 m of relief.

Input Digital Databases

Nine 7.5-minute quadrangle (30-m resolution) digital elevation models (DEMs) were acquired from the USGS. They covered a 3 by 3 mosaic of quadrangles. This mosaic covers most of the area of **QP**, but does not extend to its margins, as shown in Figure 1. The mosaic is offset to the southwest corner of **QP**. The DEM mosaic covers an area of 104° 52′ 30″ W to 104° 30′ W longitude and 32° 22′ 30″ to 32° 45′ N latitude.

A qualitative study of noise versus the true topography (as defined by paper copies of the quadrangles) was performed for each of the nine 7.5-minute quadrangles. Three of the quadrangles had signal-to-noise ratios visually estimated to be approximately 2:1 or 1:1. However, six of the quadrangles had ratios of about 1:2, with the noise being more pronounced then the original data. Because the noise on these DEMs will generate spurious valleys and slopes, they are, as is, almost useless for the NODES program. The detected valleys and slopes would be approximately the same size and magnitude as the noise. Therefore, the first task was to try to identify the optimal method for removing or abating this noise problem using noise reduction methods. Studies with

Fourier filters indicate that the noise does not have a regular enough repeat frequency that it can be simply filtered out, without introducing aliasing effects. Fourier filters were therefore deemed to be inappropriate for removal of the noise from these DEMs. Several square filters were evaluated. An 11 by 11 smoothing filter was the optimal one and removed a considerable amount of the east-west noise as displayed with a difference image between the original and the cleaned topography. Smaller filters left too much noise, and larger ones averaged out actual topographic features, without removing appreciably more noise.

The Hobbs region and **QP** detailed area overlap the boundary between two adjacent Thematic Mapper (TM) scenes. The northern scene, path 31 and row 37, was acquired on 20 December 1982, and the southern, path 32 and row 37, on 24 September 1985. VICAR was used to register the northern and southern images to base maps, mosaic them, and resample them to the 30-m resolution of the DEM data. The color balance between the northern and southern images was adjusted so that the boundary was as transparent as possible visually. A color composite using TM bands 7 (red), 4 (green), and 2 (blue) was generated for manual lineament analysis and display. Visual comparisons were made to select which TM band to use in the testing of NODES. Band 2 tends to show fewer details than the other two. Band 4 and 7 show a similar amount of features; however, band 4 displays more of the road systems and other cultural noise; therefore, band 7 was selected as the one to analyze.

Nodes Program Operation

Detection of Valleys

The NODES program superimposes a circular kernel detector onto the topography in order to find valleys and topographic gradients that may be fault or fracture controlled. One can select a variety of detector sizes, ranging from 3 to 91 pixels in diameter. A discussion of the three-pixel valley detector will illustrate the concepts of the NODES program. The circle reduces to a 3 by 3 square, and is identical to Jenson's (1985) and Qian et al.'s (1990) valley detector. The detector examines each 3 by 3 block of elevation points in the DEM. It tests four different directions, from point 1 to 1′, 2 to 2′, 3 to 3′, and 4 to 4′. If the center point (C in the section below) is topographically lower than both end points in one of the four look directions, then the point is a valley. Because one is comparing points on the edges to the center point, the north-south and east-west distances in this example will be one grid point (30 m) on each side of the center. This 3 by 3 detector is therefore testing for valleys 60 m across.

	1	2	3
Look directions for a	4	C	4′
three-pixel detector:	3′	2′	1′

NODES forms the detectors by mathematically drawing a circle within a box, as shown in Figures 2a and 2b. The user specifies the diameter of the circle and how thick (inner to outer radii) the circle is to be. The detector used by Eliason (1984), Eliason and Eliason (1985), and Eliason and Thiessen (1987) is a seven-pixel NODES circle. The NODES program then identifies (with ones) all points that lie within the circle. It flags all other points with zeroes. If there is unequal pixel spacing in the north-south and east-west directions, then NODES adjusts the detector accordingly so that the circle may be 7 pixels wide and 5 pixels high. The detector examines the digital topography. Each DEM grid point within the circular detector is tested against its symmetrically opposite point. If both end points are higher than the center by a user input threshold depth, then the detection is successful. All
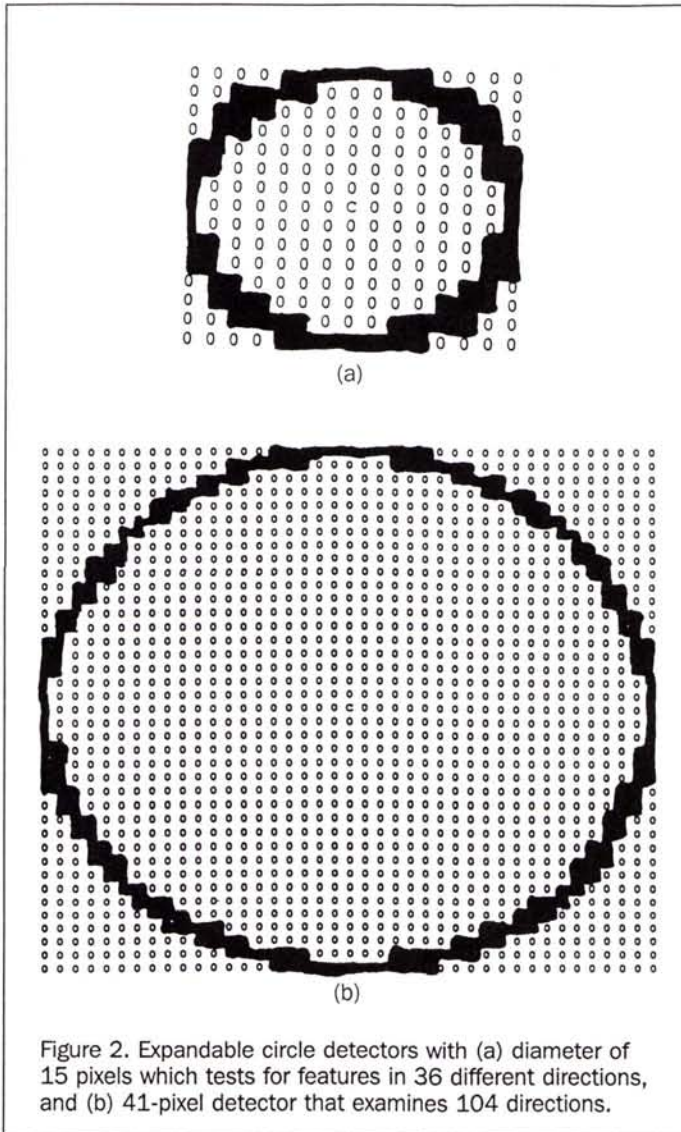
(a)

(b)

Figure 2. Expandable circle detectors with (a) diameter of 15 pixels which tests for features in 36 different directions, and (b) 41-pixel detector that examines 104 directions.

the gray shades on these plots. Notice that the centers of the valleys are where the highest number of detections are found, and the numbers decrease toward the side walls of the valleys. Examination of topographic quadrangle maps revealed that the northwest-oriented valleys were approximately 1200 m across, and the 41-pixel valley detector delineated them best.

Other Image and Topographic Features

The expandable circle detector can be used to find topographic slopes. One of the end points must be higher then the central point by at least the threshold value, and the other must be lower. Notice that the gradient being found is twice as steep as it might appear. A detector 11 pixels across at a resolution of 30 m per pixel will be 300 m wide. A threshold elevation difference of 3 m does not apply for this entire distance. Instead, one is checking the end points versus the central point just like the valley detector. For this example, the threshold will be over a distance of only 5 pixels or 150 m. The present study used this detector, designated 11G (gradient) which searched in 26 directions. Figure 4a shows the results applied to **GR**.

A number of lineament features can be found automatically by applying the NODES routines to TM image data, spe-
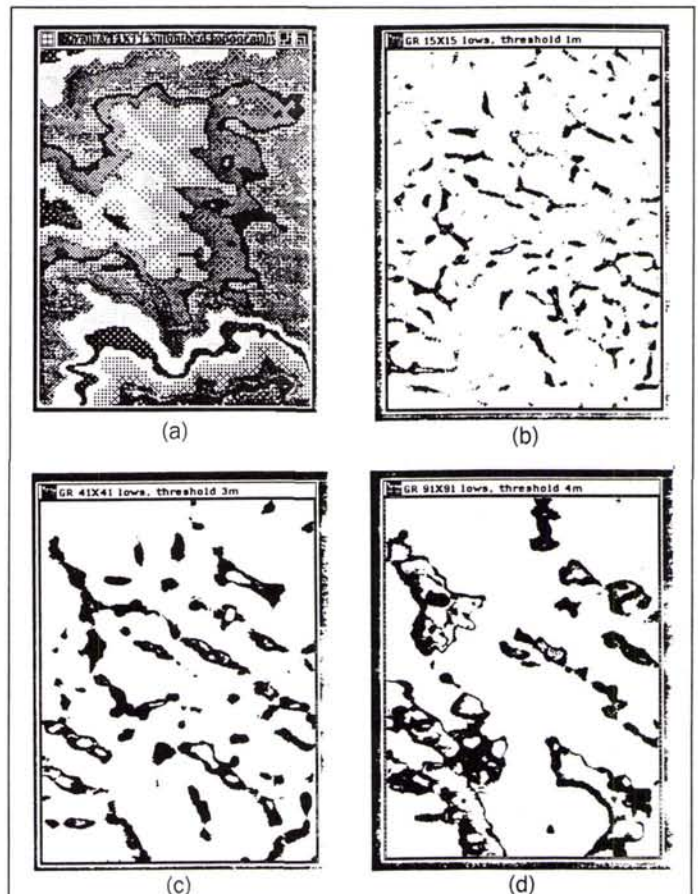

(a)

(b)

(c)

(d)

Figure 3. (a) Gray shade topography for GR area. (b) Valley bottoms found with the 15-pixel detector shown on Figure 2a. The central low point of the valley had to be at least 1 m lower then the side walls. (c) Valleys 41 pixels wide and 3 m deep, found with the detector of Figure 2b. (d) 91-pixel wide valleys at least 4 m deep.

kernel directions, defined by opposite pairs of ones within the circle, are tested. The number of directions for which the threshold condition is satisfied is tallied and indicates how well formed the valley is.

In order to determine the proper detector size and threshold to use in a study, one has to try several different combinations and select the option that gives the most reasonable results. The in-depth-study area, Grama Ridge (**GR**), was created which included the northwest oriented valleys that were one of the major targets of this investigation. The topography of **GR** is shown in Figure 3a. Three runs with different size valley detectors were processed, as shown in Figure 3. Figure 3b shows valleys that are 15 pixels (420 m) in width and must be at least 1 m deep to be found with the detector of Figure 2a. This filter, designated 15L (for lows), tests in 36 directions. Valleys 41 pixels (1200 m) across with threshold depths of 3 m are plotted on Figure 3c. This detector, 41L, is shown on Figure 2b, and tested 104 directions for valley low points. 91-pixel (2700 m) wide, 4-m depth valleys are shown on Figure 3d. The 91L detector examined 228 directions. The number of directions for which the valley node is deeper than the threshold depth is tallied and plotted as
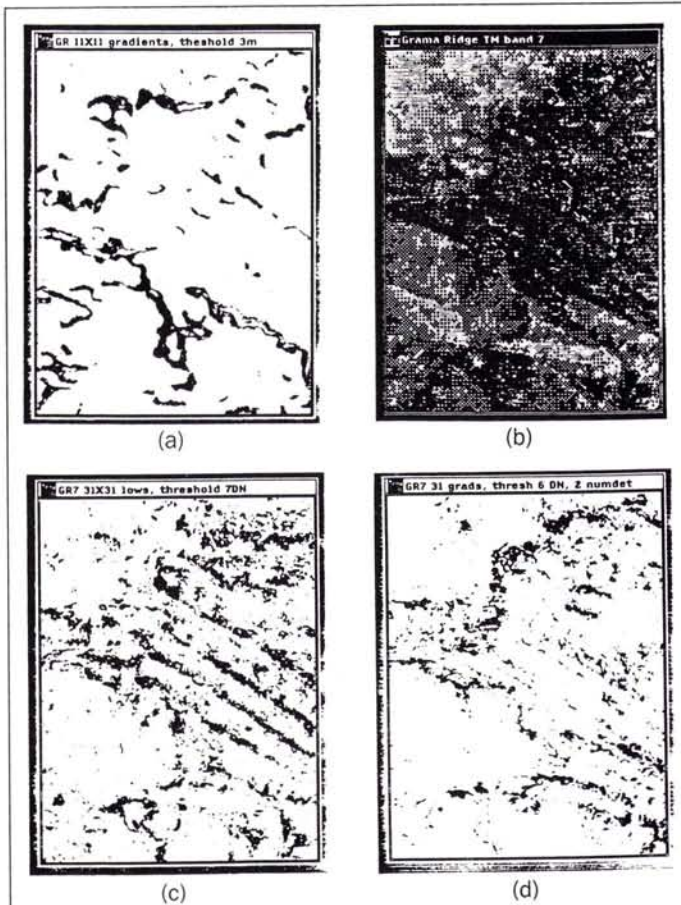
Figure 4. (a) 3-m topographic gradients detected in GR using an 11-pixel detector. (b) Gray shade image of Landsat Thematic Mapper band 7. (c) Darker zones found on TM band 7 with a 31-pixel diameter kernel. The lows had to be at least 7 DN values less than the surrounding data points. (d) Rapid gradients found in GR using a 31-pixel diameter detector applied to TM band 7. The gradients had to exceed 6 DN and be found at least two directions in the circle.

cifically TM band 7 for this study (Figure 4b). The valley detector can be directly used to find darker features on an image. In this case, the threshold value is not a depth in metres, but is instead how different the DN value (digital number) of the center point is with respect to the ends. The DN value is a measure of the gray scale intensity of each image pixel point. It usually ranges from 0 (dark) to 255 (light). Results from a 31-pixel wide kernel (detector 31L) in which the dark zones had to be 7 DN values darker to be counted are plotted on Figure 4c. Eighty directions were tested.

Rapid gradients in images (places where they change colors or brightness) were detected by using the topographic slope detector applied to the image data. Figure 4d shows results using a 31-pixel gradient detector with a threshold slope value of 6 DN applied to TM band 7. Any point must be found in at least two look directions to be included on this plot. This detector was designated 31G and examined 80 directions.

The routine has been modified so that topographic ridges or bright zones on images can be found with the varia-

ble size detector. One simply checks to see if the central point is higher (topographically or DN value) than both ends by an amount greater than the threshold value. This option was not used in the present study, although it could be utilized to find lineaments that are displayed as lighter linear features as well as ridge lines.

Manual Study of Databases

This report used two pre-existing hard copies of TM images for lineament studies. The first was the "northern" image at a scale of 1:250,000. The "southern" image was studied at 1:192,000 scale. Lineaments were manually identified on these based on color and tonal patterns and other standard lineament identification methods. There is a small amount of overlap between the southern and northern images, and some lineaments were identified on both. Figure 5a shows these lineaments for the **QP** area. The Grama Ridge in-depth-study area is indicated with a heavy line on this figure.

A number of subsurface structural contour maps are available for the study area, and are listed in Table 1. This table also summarizes non-stratigraphic databases that were analyzed for this report. Haigler and Cunningham (1972)

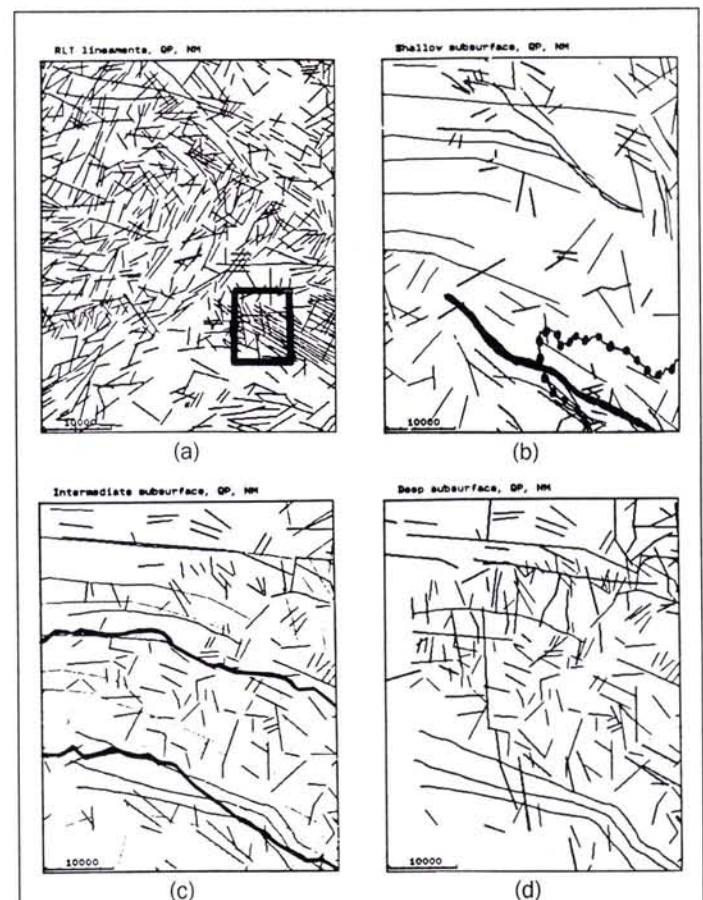Figure 5. (a) Surface lineaments mapped in the Querecho Plains (QP) area. The bold rectangle is the GR study area. (b) Shallow subsurface linears (S on Table 1) mapped for QP. The heavy line is the axis of the San Simon Swale extension (SSS) and the solid/dot line is the edge of Tertiary basins. (c) Intermediate (I) depths subsurface linears. The Capitan Reef is highlighted. (d) Deep (D) subsurface linears. All scales are in metres.

TABLE 1. STRATIGRAPHIC HORIZONS AND OTHER FEATURES USED IN THIS REPORT. WHEN NOT SPECIFIED, THE TOP OF THE HORIZON WAS MAPPED. LINEAMENTS (L) ARE SHOWN ON FIGURE 5A. SHALLOW DEPTH FEATURES (S) ARE PLOTTED ON FIGURE 5B. INTERMEDIATE (I) AND DEEP (D) FEATURES ARE MAPPED ON FIGURES 5C AND 5D, RESPECTIVELY. TOPOGRAPHIC SCARPS, TERTIARY MAFIC DIKES, EDGES OF TERTIARY BASINS, MARGINS OF THE CAPITAN REEF, AND SILURIAN/DEVONIAN GRADIENTS ARE AS MAPPED BY THE SOURCES IN TABLE 1. ALL OTHER FEATURES WERE VISUALLY IDENTIFIED DURING THE PRESENT STUDY.

Lithologic Layer or Other	Depth	Source
TM image lineaments	L	This study
Topographic scarps	S	Hendrickson and Jones (1952), Nicholson and Clebsch (1961), Ash (1963)
Tertiary basin margins	S	Baumgardner et al. (1982)
Tertiary mafic dike	S	Calzia and Hiss (1978)
Groundwater table	S	Ash (1963)
Bedrock highs	S	Ash (1963)
Post Mesozoic erosion surface	S	Ash (1963)
Top of undifferentiated Redbeds	S	Nicholson and Clebsch, (1961)
Rustler formation	S, I	Hiss (1976B)
Salado salt	S, I	Hendrickson and Jones (1952)
Castile salt	S, I	Anderson and Powers (1978)
Capitan reef margin and low zones	I	Hiss (1976A)
Yates	I, D	Conoco staff
Wolfcamp	D	Conoco staff
Silurian/Devonian	D	Haigler and Cunningham (1972)

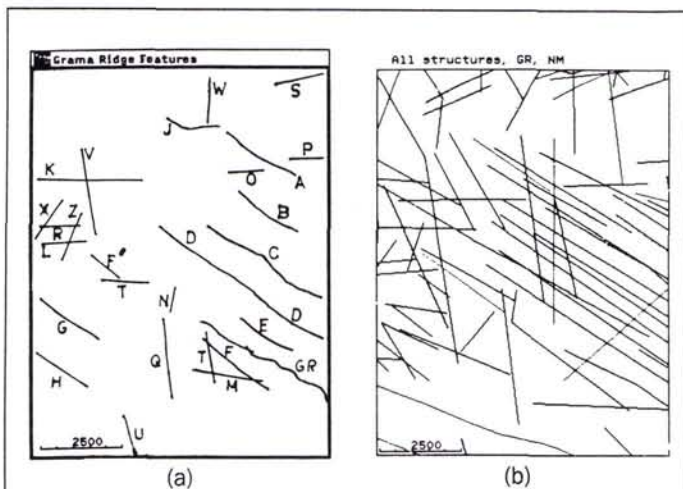(a)   (b)

Figure 6. (a) Topographic and imagery features that will be discussed for the Grama Ridge (GR) in-depth-study area. Features A through H are the northwest-oriented valley lineaments that were one of the initial targets of this study. GR is the topographic scarp called Grama Ridge. (b) Lineaments and subsurface linears (top of the Red Beds, Yates, Wolfcamp, and Rustler levels, lows in the Capitan reef) mapped in GR. The scale bars are in metres.

identified subsurface faults on the Silurian/Devonian. All of the rest of the depth maps were photo reduced to 1:250,000 scale, and linear gradients were identified visually. These gradients could be simply sharp monoclinal features. Conversely, they may represent fault offsets, particularly where the well control is sparse. In order to compare these to the other fault and fracture data, the selected gradients were digitized, and are plotted on Figures 5b, 5c, and 5d. The Yates structural contour map shows a major gradient in the southern part of **QP**. This was designated as three west-northwest gradients in the southern part of Figures 5c and 5d, one through the middle of the gradient, and one on either margin. This major gradient approximately aligns with the Capitan reef, which is accented on Figure 5c.

One of the major observations concerning Figures 5a through 5d is that the number of surface lineaments that are mapped on Figure 5a is significantly higher than any of the subsurface data. This is simply due to the resolution scale of the databases. The resampled Landsat TM data have a pixel resolution of 30 m, and so there is a data point every 30 m in the east-west and north-south direction. This is also the resolution of the USGS digital elevation models. Conversely, subsurface structural contour maps depend upon much more widely spaced input data, such as individual drill holes and (sometimes) seismic reflection profiles. These may have a spacing of, at best, 1 km, and usually a much worse spacing. As a result, the data have much worse resolving power then the TM image, and so the identified features will be much fewer. Their locations are also much more poorly constrained.

Northwest-Oriented Valleys

Observations

The Hobbs region was initially suggested as a possible site for a NODES study, partly because of the presence of a series of well defined northwest-oriented lineaments. The Grama Ridge (**GR**) in-depth-study area was selected to allow for a more complete analysis of these features. An examination of a 1:250,000-scale topographic sheet (USGS, 1973) revealed that these lineaments were paralleled by low valleys. Detailed topographic sheets at 1:24,000 scale show these valleys to be approximately 1 km wide and 6 to 10 m deep. The valleys to the north tend to have steeper southwest sidewalls. These features were designated as valleys **A** through **H**, as indicated on Figure 6a. They were compared to each of the products from NODES (Figures 3 and 4) and to the visually identified lineaments and subsurface features mapped in Figures 5 and 6b. Subsurface gradients in **GR** include ones picked off the top of Redbeds, the Rustler and Yates formations, and the Wolfcamp stratigraphic interval.

The northwest-oriented lineaments are tonal ones, being defined by well developed elongate zones of darker pixels. One of the coherent patterns that emerged from this analysis was that this dark zone was always offset to the southwest from the valley bottom. The one exception was valley **F'**, which is a very short valley in a complex zone, so its relationships are not entirely clear. This dark zone offset could be due to several different factors: (1) This may be caused by a relatively low sun angle with the sun to the southwest preferentially shading these slopes. The TM data are a mosaic between a southern scene, acquired in September, and a northern one, imaged in December. More lineaments have been visually selected on the northern image, including the northwest-oriented valley lineaments. However, the amount of darkening appears somewhat extreme considering the gentle slopes that are present. (2) There may be a coherent change in vegetation from south to north slopes because of slightly cooler and damper conditions on the northward facing slopes. (3) The change may be due to lithologic variations. Maps of the area (Barnes, 1976; Hunt, 1977) show the bedrock to be the Tertiary aged Ogallala Formation with caliche caps. The valley bottoms themselves are mapped as either windblown sand or alluvial deposits. Neither map in-

dicates different lithologies to the southwest of the valleys, although there could be sand drifting into this position due to winds from the southwest. Conversely, a dark layer or layers within the Ogallala Formation may be offset and exposed at each location. (4) For most of the valleys (**A, B, C, D, F'**, and **G**) the southwest side is steeper, and so the dark zone might be soil variations responding to changes in slope angle. However, valley **E** is symmetric, and valleys **F** and **H** actually have steeper northeast slopes. (5) There may be a coherent set of fault scarps forming the southwest side of each valley. The fault offsets could then expose deeper portions of the Ogallala, including different lithologies and/or layers below the caliche cap. One argument against this is that the southwest slopes are usually, but not always, the steepest, as one would expect for faulting of this nature.

A generalized pattern was observed for a northeast to southwest traverse across the valleys. The dark zone on the image is to the southwest of the valley bottom itself, as discussed above. Lineaments were visually identified at the northeast and southwest margins of this dark zone. The dark zone was delineated with detector 31L, and with rapid gradients in the image found with detector 31G at both of its edges. This package in its entirety was observed for valley **B**, and nearly so for **A**, although only the southwest 31G and lineament zone was well developed for the latter example. For most valleys, including **C, D**, and **E**, this lineament package was offset so that the valley bottom and the northeast lineament zone overlapped. Valley **F** showed 31L along the valley bottom. The 31L and 31G are also defining a crossing feature of some sort. Valley **F'** has the 31L to the northeast, with small patches of 31G about it. Valley **G** shows the double lineaments to the southwest with one along the valley itself, but no 31L or 31G. A scattered response for 31L to the southwest and lineaments to the northeast and southwest of the valley are exhibited by valley **H**.

Origin of the Valleys
Initially, there was a question as to whether the valleys were structurally controlled, or if they are just elongate wind-blown sand deposits. The 1:250,000-scale geologic map of the region (Barnes, 1976) shows the lineaments to be underlain by Pliocene aged Ogallala Formation (part of the Plano Estacado). However, the valleys are filled by Recent wind-blown sand deposits. A few of the valleys contain small playa lakes (Barnes, 1976). A surficial geologic map at 1:500,000 scale (Hunt, 1977) shows the valleys as being floodplain and channel deposits along generally dry arroyos and washes. The surrounding lithology is moderately thick (1 to 3 feet) sand on caliche capping the Ogallala Formation.

Arguments for structural control of the northwest valleys are numerous. Subsurface maps of the Yates, Wolfcamp, Salt, and Rustler indicate some well defined northwest-oriented gradients close to **GR**, and a few poor ones within the area itself. The Capitan reef (Figure 5c) lies directly under these valleys (Hiss, 1976a) and is parallel to their trend at this location. The valley lineaments are thought to be due to a drape structure cored by the reef accentuated by salt dissolution. This is supported by the fact that the northern valleys have steeper south slopes, indicating normal faults down dropping to the north (assuming the scarps are not fault line scarps). The Grama Ridge (**GR** on Figure 6a) is approximately one-third of the distance from the southern edge of the reef and downdrops structures to the south.

A field check of some of the features in the Hobbs region included examination of several of the major northwest valley lineaments. The most accessible one was east of **GR** and, for that matter, of the Querecho Plains detailed study area. The feature is within the Hobbs project area, and lineaments

parallel to the valley were identified in the regional study. The valley straddles the corners of sections 15, 16, 21, and 22 of township R35E, T21S. The topographic map shows that the valley is asymmetric, with the southwest side being somewhat steeper than the northeast side. The valley is a contact between Quaternary aged sand (Barnes, 1976) on the northeast side and Tertiary Ogallala Formation with a caliche cap to the southwest. In the field, this contact was observed to be in the bottom of the valley and extremely sharp and linear, and so was assumed to be fault controlled with the sand occupying the down-dropped side.

The San Simon Swale (heavy line on Figure 5b) aligns with the Capitan reef's southern edge (Hiss, 1976a), and was formed by extensive dissolution of evaporites, as noted by Baumgardner et al. (1982). They observed that salt dissolution leads to well developed Tertiary basins, mapped on Figure 5b. The removal of this volume of evaporites will allow the adjacent salt and overlying lithologies to expand laterally into this zone. The overlying lithologies will break in a brittle manner into a series of parallel extensional grabens, as shown by the Rustler formation (Hiss, 1976b). When these extensional structures reach the surface, they generated the northwest-oriented valley lineaments studied in **GR**. The extension of the San Simon Swale (SSS) to the northwest is displayed as a discontinuous zone with the 15L and 41L detectors. This zone is very well defined and continuous on the 91L plot. A field check of the SSS graphically illustrates why it was found best with the widest detectors. It is a very gentle, wide valley several kilometres in width with a relatively flat bottom.

There are several excellent analogs of this type of behavior in the southwestern United States. Dissolution of salt anticlines in Arches National Park, Utah, has a pronounced control on formation of parallel joint systems (Doelling, 1985; Chronic, 1988; 1990; Baars, 1989; Phillips, 1992; Thiessen, 1992, unpublished data). Evaporite layers at depth have formed elongate salt domes (often initialized and localized by basement faults). As these structures migrated towards the surface, they bent the overlying rocks into anticlines. When the salt neared the surface, it was dissolved by groundwater, causing a void, as expressed by a physical valley (Salt and Cache valleys). The surrounding salt and overlying lithologies laterally expanded and collapsed into this void, causing the upper brittle sandstone layers to break into a series of joints parallel to the valleys and anticlinal cores. These joints controlled the location of the rock fins that often eroded into the spectacular arches of the park.

Other Features in QP
The region within which the northwest-oriented valleys and lineaments lie is truncated on the northern end by a major topographic gradient labeled **J** on Figure 6a. This feature is characterized by a strong topographic slope identified by 11G (Figure 4a) that changes from an east-west orientation to a west-northwest one. A patchy dark zone on the image, found with 31L, trends east-west just south of **J**. **J** sits within an east-west 31G band. A small quarry adjacent to the slope exhibited several west-northwest fracture orientations, paralleling the orientation of the slope, **J**, at that location. One fault displayed slickensides (plunging 70° W, north side down), indicating a predominantly normal faulting mode in the same sense of offset as slope **J** itself.

The topographic rise called Grama Ridge (**GR** on Figure 6a) forms the northeast margin of valley **F**. It forms the northern edge of the patch of valley nodes found with filter 91L (Figure 3d). It is a very well defined gradient on 11G (Figure 4a) and is paralleled by a lineament. There is a small zone of nodes found with 31L on the west end and 31G in

the eastern portion. It was mapped as a topographic scarp on 1:250,000-scale maps, as shown on Figure 5b.

The Mescalero Ridge is a major topographic scarp in the northeast region of **QP**. It is the edge of the Plano Estacado, and correlates to gradients in the Redbeds and post-Mesozoic erosional unconformity, as well as lineaments. Features found with the NODES program include topographic slopes 11 pixels in size and TM band 7 dark lineaments and gradients, both 31 pixels across. Structures appear to wrap from the northwest orientation of the Mescalero Ridge into a more west-northwest trend exhibited by graben structures in the northwest corner of **QP**. The location of the bend migrates to the north as one moves up in stratigraphy. This progressive relationship can be seen for the Yates, Rustler, Redbeds, Post Mesozoic erosional unconformity, and topographic scarps, in stratigraphic order.

All of these features discussed in this section show a basic concept in lineament and structural analyses. No feature shows up on all available databases. Therefore, one has to examine a wide variety of databases before a complete set of possible fault and fracture systems can be generated.

Structural Trends

The NODES program does have the capability of thinning the patches of lineament nodes into a single line of data points and then connecting them into chains of node points. In essence, one is automatically finding lineaments using this technique. The valley bottoms shown in Figures 3b, 3c, and 3d were processed into computer lineaments to be input into WSU's LINEAMENTS program (Thiessen, 1986; Pitz and Thiessen, 1986; Thiessen et al., 1987; 1989; 1992; Johnson, 1988; Thiessen and Rieken, 1993). The program is used to define structures that correlate spatially in plan view, as well as examine trends of structures using rose diagrams and maps of rose diagrams sampling the study area. Contour maps can be prepared showing the spatial density of surface or subsurface structures for either all orientations, or a selected range of trends.

The lineament contouring capabilities have been applied to three different data sets. The first are the lineaments shown on Figure 5a. The subsurface structures of Figures 5b, 5c, and 5d minus surface scarps were also used. The lineaments derived from the valleys detected with the three runs of NODES (Figures 3b, 3c, and 3d) were the third database. When one looks at all trends, the contour plots of lineaments had a maximum peak over the area of the northwest-oriented lineament valleys (**NW**). Secondary peaks included the Mescalero Ridge (**MR**) and an east-west (**CEW**) zone in the center of **QP**. Minor peaks were expressed in the Nash Draw (**ND**) area in the southwest corner of **QP** and a northern zone of east-west structures (**NEW**). The NODES detected valleys had a maximum on **ND**, with secondary peaks on **NW** and CEW. Subsurface structures showed the San Simon Swale (SSS) which is the southern edge of the Capitan reef, NEW, and a number of other structures as major peaks. **MR** was a more minor concentration. If one only looks at east-west oriented structures (75° to 105° trends), then the surface lineaments show major concentrations at the SSS, CEW, and a minor peak at NEW. The NODES valleys show the CEW, ND, and SSS well. Subsurface features show NEW best, CEW lesser, and **ND** as a more minor peak. Contouring only northwest trends (105° to 145°) for the lineaments plot (Figure 5a) shows a peak for **NW**, and a minor peak for **MR**. NODES defined valleys show the **NW** area first and SSS second, but do not accentuate **MR**, because it is a topographic ridge. Subsurface structures have a maximum concentration over SSS, second over **MR**, and third over **NW**. These contouring results reveal that a number of structural zones are being repeatedly found in the three

independent data bases, indicating that these are real geologic structures.

Three-Dimensional Methods

Washington State University and the Pacific Northwest Laboratories are developing program packages that determine the full three-dimensional orientations (strike and dip) and locations of possible fault and fracture planes. The computer lineaments defined by NODES are actually vectors because each node point has a location and an elevation. These can be input into the COPLANARS program package (Eliason, 1984; Eliason and Eliason, 1985; Eliason and Thiessen, 1987; Thiessen et al., 1989; Foley et al., 1988; 1990; 1992; Beaver et al., 1992; Neves and Thiessen, 1993). Vectors that lie within the same plane may be controlled by a fault or fracture. Large populations of coplanes can be examined using statistical analysis methods (Foley et al., 1990; 1992). COPLANARS was applied to the NODES detected valleys from **QP**. No good three-dimensional relationships could be observed due to the extremely low topographic relief. Future plans call for assigning elevations to the lineaments and subsurface structures in order to make them into vectors and inputting all three databases into COPLANARS.

Point data, such as seismic foci or borehole intersections of faults and fractures, can be interpreted using WSU's SEISPLN package (Rieken, 1985; Rieken and Thiessen, 1992; 1993; Thiessen and Rieken, 1993). No point data were available for the Hobbs region for SEISPLN, so it was not run.

Conclusions

The preliminary tests presented in this report show that the expandable circle lineament detector of the NODES program provides invaluable data in the Hobbs, New Mexico project area. Topographic and image features that are too wide to be detected with smaller kernals can be delineated using larger diameter circles. The routines, which have been previously utilized in areas of relatively high topographic relief, have been shown to yield excellent structural data in the extremely low relief portions of southeastern New Mexico. The NODES program has a number of advantages over other lineament detection routines in that it can be geared to the size of the features. Being a circle means it is non-directional. However, it is slower than other routines because of the larger numbers of calculations. On a 5 year old MicroVAX II, processing for small to medium detectors is shorter than manual lineament picking and digitizing. Larger detectors take a longer time. However, manual lineament studies are degraded by multiple interpreters generating different lineament populations (Thiessen et al., 1987; 1992; Thiessen and Rieken, 1993).

Northwest-oriented valleys were best defined using medium sized circles applied to digital topography. These valleys are paralleled by dark lineaments offset to the south, found with NODES using TM band 7. Visually identified lineaments were picked at the edges of the dark zones. The San Simon Swale to the southwest has been hypothesized to be caused by salt solution controlled by the southern margin of the Capitan reef. This dissolution allowed the area to the northeast to expand laterally, forming the normal faults that generated the valley lineaments. The San Simon Swale itself was found with a circular detector 91 pixels across.

Topographic scarps were readily found with the NODES detector. One corresponded to a small fault observed in an adjacent quarry. This feature was also a NODES dark lineament and gradient on TM band 7. The Grama and Mescalero ridges, previously mapped scarps, were found with NODES as topographic gradients and image lineaments. The Mescalero

ridge corresponded to gradients in four subsurface stratigraphic levels.

Contour plots of lineaments, NODES defined valleys, and subsurface structures reveal the northwest lineament valleys, Mescalero ridge, San Simon Swale, and several other major structures, particularly when one examines specific orientation trend ranges.

The expertise gained in this study should be directly applied to adjacent areas as well as similar low relief study areas. The lineament detection routines of the NODES program will allow future users to identify features of virtually any size, including very subtle features on topographic and image databases.

References

Anderson, R. Y., and D. W. Powers, 1978. Salt Anticlines in Castile-Salado Evaporite Sequence, Northern Delaware Basin, New Mexico, *New Mexico Bureau of Mines and Mineral Resources, Circular 159*, pp. 79–83.

Ash, S. R., 1963. *Ground-Water Conditions in Northern Lea County, New Mexico*, U.S. Geological Survey, Hydrologic Investigations Atlas HA-62, 1:250,000 scale.

Barnes, V. E., 1976. *Hobbs Sheet*, Bureau of Economic Geology, Geologic Atlas of Texas, 1:250,000 scale.

Baars, D., 1989. *Canyonlands Country: Geology of Canyonland and Arches National Parks*, Canyonlands Natural Historical Association, Moab, Utah, 140 p.

Baumgardner, R. W., Jr., A. D. Hoadley, and A. G. Goldstein, 1982. *Formation of the Wink Sink, a Salt Dissolution and Collapse Feature, Winkler County, Texas*, Bureau of Economic Geology, Report of Investigations 114, 38 p.

Beaver, D. E., J. R. Eliason, and R. L. Thiessen, 1992. Regional Digital Analysis of Major Crustal Structures in Washington State, *Proceedings of the Seventh International Conference on Basement Tectonics*, pp. 329–340.

Calzia, J. P., and W. L. Hiss, 1978. Igneous rocks in northern Delaware basin, New Mexico and Texas, *New Mexico Bureau of Mines and Mineral Resources, Circular 159*, pp. 39–45.

Chronic, H., 1988. *Pages of Stone: Geology of Western National Parks and Monuments, Vol. 4, Grand Canyon and the Plateau Country*, The Mountaineers, Seattle, Washington, 158 p.

———, 1990. *Roadside Geology of Utah:* Mountain Press Publishing Corp., Missoula, Montana, 326 p.

Doelling, H. H., 1985. *Geology of Arches National Park*, Utah Geological and Mineralogical Survey Map 74, 15 p.

Eliason, J. R., 1984. *A Technique for Structural Geologic Analysis of Topography*, Ph.D. thesis, Washington State University, Pullman, Washington, 166 p.

Eliason, J. R., and V. E. Eliason, 1985. A Comparative Study of Fracture Planes Computed from Topography and Lineaments from Imagery with Structures and Mineralization in the Magnesite Belt of Washington State, *Proceedings of the Fourth Thematic Conference on Remote Sensing for Exploration Geology*, pp. 655–664.

Eliason, J. R., and R. L. Thiessen, 1987. Geologic Spatial Analysis, a New Multiple Data Source Exploration Tool, *Proceedings of the Fifth Thematic Conference on Remote Sensing for Exploration Geology*, pp. 763–774.

Foley, M. G., D. E. Beaver, M. A. Glennon, T. H. Mroz, J. R. Eliason, and R. L. Thiessen, 1988. Application of Remote Geologic Analysis to Gas Exploration in West Virginia, *Geological Society of America, Abstracts with Programs*, Vol. 20, p. A229.

Foley, M. G., P. G. Heasler, and R. L. Thiessen, 1990. *Application of Remote Geologic Analysis to Gas Exploration in Devonian Shale*, Unpublished report to Department of Energy's Morgantown Energy Technology Center, 320 p., 20 plates.

Foley, M. G., K. A. Hoover, P. G. Heasler, N. J. Rynes, and R. L. Thiessen, 1992. Automated Geomorphic Pattern-Recognition for

Morphotectonic Analysis, *American Geophysical Union Chapman Conference on Tectonics and Topography*, p. 20.

Haigler, L. B., and R. R. Cunningham, 1972. *Structure Contour Map on Top of the Undifferentiated Silurian and Devonian Rocks in Southeastern New Mexico*, U.S. Geological Survey, Oil and Gas Investigations Map OM-218, 1:250,000 scale.

Hendrickson, G. E., and R. S. Jones, 1952. *Geology and Ground-Water Conditions of Eddy County, New Mexico*, New Mexico Bureau of Mines and Mineral Resources, Ground-Water Report 3, 169 p.

Hiss, W. L., 1976a. *Structure of the Permian Guadalupian Capitan Aquifer, Southeast New Mexico and West Texas*, New Mexico Bureau of Mines and Mineral Resources, Resource Map 6, 1:500,000 scale.

———, 1976b. *Structure of the Permian Ochoan Rustler Formation, Southeast New Mexico and West Texas*, New Mexico Bureau of Mines and Mineral Resources, Resource Map 7, 1:500,000 scale.

Hunt, C. B., 1977. *Surficial Geology of Southeast New Mexico*, New Mexico Bureau of Mines and Mineral Resources, Geologic Map 41, 1:500,000 scale.

Jenson, S. K., 1985. Automated Derivation of Hydrologic Basin Characteristics from Digital Elevation Data, *Proceedings of Auto-Carto 7, Digital Representations of Spatial Knowledge*, pp. 301–310.

Johnson, L. K., 1988. *Computer Analysis of Remote Sensing and Geologic Datasets*, M.S. thesis, Washington State University, Pullman, Washington, 215 p.

Neves, D. S., and R. L. Thiessen, 1993. The Three-Dimensional Recognition of Active Faults and Range Front Faults Using Digital Elevation Models, *Proceedings of the Ninth Thematic Conference on Geologic Remote Sensing*, pp. 1029–1040.

Nicholson, A., Jr., and A. Clebsch, Jr., 1961. *Geology and Ground-Water Conditions in Southern Lea County, New Mexico*, New Mexico Bureau of Mines and Mineral Resources, Ground-Water Report 6, 123 p.

Phillips, M., 1991. *Geology: Arches National Park:* Canyonlands Natural History Association, Moab, Utah, 8 p.

Pitz, C., and R. L. Thiessen, 1986. Lineament Analysis and Structural Mapping of the Trans-Idaho Discontinuity and Their Implications for Regional Tectonic Models, *Proceedings of the Sixth International Conference on Basement Tectonics*, pp. 16–24.

Qian, J., R. W. Ehrich, and J. B. Campbell, 1990. DNESYS - An Expert System for Automatic Extraction of Drainage Networks from Digital Elevation Data, *IEEE Transactions on Geoscience and Remote Sensing*, Vol. 28, pp. 29–45.

Rieken, E. R., 1985. *Computer Generated Fault Surface Determinations from Earthquake Foci, Washington State, 1969-1983*, M.S. thesis, Washington State University, Pullman, Washington, 126 p.

Rieken, E. R., and R. L. Thiessen, 1992. Three-Dimensional Model of the Cascadia Subduction Zone Using Earthquake Foci, Western Washington, *Bulletin of the Seismological Society of America*, Vol. 82, pp. 2533–2548.

———, 1993. Three-Dimensional Fault Surface Models for the Loma Prieta Aftershock Sequence, *Proceedings of the Ninth Thematic Conference on Geologic Remote Sensing*, pp. 1015–1026.

Thiessen, R. L., 1986. LINMNT, Lineament Analysis, National Association of Geology Teachers Special Publication, *Computer Software Designed for Use in Undergraduate Education*, pp. 183–187.

Thiessen, R. L., J. R. Eliason, and E. R. Rieken, 1989. Three-Dimensional Computer Analysis and Modeling of Remote Sensing-Structural Geologic Problems, *1989 International Geoscience and Remote Sensing Symposium (IGARSS '89)*, pp. 89–92.

Thiessen, R. L., L. K. Johnson, H. P. Foote, and J. R. Eliason, 1987. Surface Reflectance Correction and Stereo Enhancement of Landsat Thematic Mapper Imagery for Structural Geologic Exploration, *Proceedings of the Fifth Thematic Conference on Remote Sensing for Exploration Geology*, pp. 763–774.

Thiessen, R. L., and E. R. Rieken, 1993. Delineation of Active Crustal

Faults in Western Washington Using an Integrated Remote Sensing Approach, *Proceedings of the Ninth Thematic Conference on Geologic Remote Sensing*, pp. 239–250.

Thiessen, R. L., E. R. Rieken, and D. S. Neves, 1992. The Use of Stream Drainage Networks in a GIS Program Package for the De-
lineation of Geologic Faults and Fractures, *Sixth Annual GIS Symposium (GIS'92)*, Forestry Canada FRDA Report 173, pp. D2:1–11.

USGS, 1973. *Hobbs, New Mexico; Texas*, U.S. Geological Survey, Western United States 1:250,000-scale map.

Call for Papers

9TH ANNUAL GEOGRAPHIC INFORMATION SYSTEMS ISSUE

Photogrammetric Engineering & Remote Sensing

The American Society for Photogrammetry and Remote Sensing will publish its Ninth Annual Geographic Information Systems issue of *PE&RS* in November 1994. Special Guest Editors are Ann Maclean of the Michigan Technological University and Gordon Maclean of Maclean Consultants, Ltd. This issue will contain both invited and contributed articles.

Authors are especially encouraged so submit manuscripts on the following types:

- Spatial modeling of natural resources
- Assessing spatial accuracy of GIS information
- Use of GIS in remote sensing activities
- Economic issues of GIS utilization by local and county governments
- Applications of digital orthoimagery in GIS
- Integration of GIS and decision support systems
- Use of GPS in GIS

All manuscripts, invited and contributed will be peer-reviewed in accordance with established ASPRS policy for publication in *PE&RS*. Authors who wish to contribute papers for this special issue are invited to mail five copies of their manuscript to:

Dr. Ann Maclean
School of Forestry and Wood Products
Michigan Technological University
1400 Townsend Drive.
Houghton, MI 49931-1295
906-487-2030; fax 906-487-2915

Dr. Gordon A. Maclean
Maclean Consultants, Ltd.
P.O. Box 655
Houghton, MI 49931-0566
906-482-9692

All papers should conform to the submission standards in "Instructions to Authors" which appears monthly in *PE&RS*. **Manuscripts must be received by 1 February 1994 in order to be considered for publication in this special issue.**